# The formation of high surface concentrations of hydroxyl groups in the plasma polymerization of allyl alcohol

**A. P. Ameen*, R. D. Short* and R. J. Ward**
*Laboratory for Surface and Interface Analysis, Department of Engineering Materials, University of Sheffield, Sir Robert Hatfield Building, Mappin Street, Sheffield S1 4DU, UK*
*(Received 13 December 1993)*

Plasma polymers (PPs) of allyl alcohol (AA) were prepared under a range of different monomer flow rate conditions. The resultant PPs were analysed by X-ray photoelectron spectroscopy (X.p.s.) and high resolution monochromated X.p.s., with the help of trifluoroacetic anhydride (TFAA) labelling of hydroxyl groups, and time-of-flight secondary ion mass spectrometry (TOF s.i.m.s.). Emphasis was put on obtaining PPs with good hydroxyl retention, and on exploring the structure of these materials. Selected PPs were heated in argon to investigate the functional group mobility, and the level of crosslinking in these materials was evaluated by a simple washing test in distilled water. The u.v. stability was assessed on exposure to a 'black lamp'. The observed behaviour of the PPs is explained by the presence of trapped residual free-radical centres in these materials. The results reported have important implications for the use of PPs as coating materials, particularly in applications where these materials may be subjected to natural sunlight. To increase the amount of surface functionality in these polymers, the post-plasma polymerization grafting of the AA was investigated. In order to assess the importance of the double bond in the monomer, various PPs of 1-propanol were also prepared and labelled.

**(Keywords: plasma polymerization; allyl alcohol; trifluoroacetic anhydride)**

## INTRODUCTION

The plasma polymerization of organic compounds as a method to produce thin films has been a particularly active area of research[1–10]. The process offers several advantages over conventional polymer synthesis:

1. The starting monomers used do not need to contain the type of functional groups normally associated with conventional polymerization.
2. Polymerization may be achieved in a clean environment without the use of solvents.
3. Ultra thin, 'pin-hole' free films may be prepared.
4. Through careful control of the polymerization parameters, it is possible to tailor the films with respect to specific chemical functionality, thickness and other chemical and physical properties.

Unlike conventional polymers, plasma polymers (PPs) do not consist of chains with regular repeat units, but tend to form an irregular three-dimensional crosslinked network. The chemical structure may be quite different from a conventional polymer which has been derived from the same monomer. This study is concerned with the preparation and characterization of PPs which contain a high concentration of hydroxyl functionalities. Films of this type have considerable technological importance and there have been several recent reports detailing the preparation and characterization of new highly functionalized surfaces on 'inert' substrates by using glow discharge plasmas[1–9]. Gombotz and Hoffman[1] described the plasma polymerization of allyl amine and allyl alcohol (AA) on to poly(propylene-*co*-ethylene), poly(ethylene terephthalate), and silastic films to produce new surfaces containing amine and alcohol groups, respectively. These new surfaces modify protein and cell adsorption and further provide sites for the subsequent immobilization of graft polymers[2].

There is considerable interest in the structure of PPs[8–11]. Characterization of these materials, however, is not straightforward, as the process produces little material, and this is generally insoluble in most solvents (depending on the monomer, and the plasma conditions). This problem can be overcome by using surface analysis techniques, such as X-ray photoelectron spectroscopy (X.p.s.), which can provide both an elemental analysis and certain functional group information. Although the use of monochromated high resolution X.p.s. can distinguish between some functional groups better than the more usual, lower resolution, non-monochromated X.p.s., the technique is still limited by the small range of chemical shifts observed in the core levels and the overlap in binding energies of some functional groups, e.g. $\underline{C}$–O–H and $\underline{C}$–O–C in the carbon 1s (C 1s). Even with the use of peak fitting routines, X.p.s. cannot be used to unambiguously identify specific functionalities in multifunctional materials. For this reason, approaches have been developed with 'model' polymers which involve the specific 'tagging' of a functional group to aid its identification by X.p.s.[12–15]. The criteria for successful

---

*To whom correspondence should be addressed

0032-3861/94/20/4382–10

derivatization are stringent[15]:

1. The tag must undergo a specific reaction with a particular functional group and introduce a new atomic species into the surface.
2. The derivatization should proceed rapidly under mild conditions, and should go to completion.
3. Solvents (if required) should be benign.

The last two conditions are hard to meet, as solution phase derivatizations are often hindered in the polymer surface layer and solvents that permeate into the polymer are likely to give rise to surface reorganization[15]. Solvents may also extract lower-molecular-weight species from the surface. For these reasons, vapour phase derivatizations are preferred.

In this work, the plasma polymerization of AA has been studied under a range of conditions. Trifluoroacetic anhydride (TFAA) was used as a labelling agent for the hydroxyl groups to distinguish them from other $\underline{C}$–O functionalities, such as ethers, in order to investigate the degree of retention of hydroxyl groups. (TFAA is also very reactive towards epoxides[16].) The TFAA derivatization reaction is one of the most widely used for X.p.s. analysis[1,14,17], as the TFAA can be used in the vapour phase, and the reaction proceeds rapidly to completion. Considerable difficulty was encountered in obtaining a chemically acceptable fit of the C 1s core level in the TFAA labelled PPs. In our attempted fits, we used peaks for hydrocarbon ($\underline{C}$H), plus $\underline{C}$–O, $\underline{C}$=O, O–$\underline{C}$=O, O–$\underline{C}$–$CF_3$, and $\underline{C}F_3$. To obtain a better insight into this problem, the high resolution capability of the Scienta ESCA 300 spectrometer was employed[18]. The information obtained in this way was subsequently used to fit the X.p.s. data that had been obtained on the non-monochromated instrument.

For comparison, the plasma polymerization of 1-propanol, the saturated analogue of allyl alcohol (AA), has also been studied. Although this might not be expected to retain such a high percentage of hydroxyl groups as AA, other work has shown that some saturated carboxylic acids and esters retain a high degree of functionality on plasma polymerization[19,20].

The use of time-of-flight secondary ion mass spectrometry (TOF s.i.m.s.) to probe the structure in a number of PPs has recently been described[21–23]. In the secondary ion mass spectra of plasma polymerized methacrylate monomers, ions diagnostic of polymer repeat units and polymer chain-ends have been clearly identified[21,22]. It has also been shown that the intensities of these ions reflect changes in PP structure, which can be approximately correlated with retention of functional group (in this case, carboxylate). Here, TOF s.i.m.s. has been used to probe a number of plasma polymerized AA samples, which have been prepared using low, moderate and high monomer flow conditions.

The amount of material obtained in a typical polymerization is not enough for analysis using the more conventional techniques employed in polymer science (e.g. gel permeation chromatography, nuclear magnetic resonance, etc.) and, therefore, two simple tests were devised to probe the extent of crosslinking in those PPs showing the greatest and least hydroxyl retention. These materials were heated under argon to examine functional group mobility and washed in distilled water to investigate solubility.

The samples were also exposed to a low intensity u.v. source. The u.v. stability of PPs has, up until now, been rather overlooked[24], despite the known presence of free-radical centres in these materials. Elsewhere[24], we have suggested that the more aggressive the plasma conditions used to produce the materials, then the more sensitive they will be to u.v. irradiation; this hypothesis is further tested here.

## EXPERIMENTAL

### *Materials and plasma polymerization apparatus*

Allyl alcohol (AA) (Aldrich Chemical Co. Ltd) was supplied as a liquid with a purity of >99%. The experimental set-up for the plasma polymerization (shown in *Figure 1*) is essentially composed of a large tubular Pyrex reactor (internal diameter = 5 cm, length = 32 cm). All of the vacuum seals were 'grease-free' to minimize contamination. The apparatus was pumped down to a base pressure of ~0.01 torr by a double-stage rotary pump (GDR). At the start of each experiment, the leak rate of the vacuum line was determmined by closing the cold-trap valve and measuring the rise in pressure as a function of time (using the equation given in ref. 19). Only when the leak rate was low (since a relatively large amount of oxygen might be incorporated into the polymer film during polymerization), was monomer (i.e. AA) vapour allowed into the reactor, through the needle valve, to the desired pressure. The flow rate of the monomer vapour (*F*) was then measured in the same way as the leak rate. After this operation, the cold-trap valve was opened and the radio frequency (r.f.) power (10 W) at 13.56 MHz (supplied from an RF generator, model GPS 100 RF/Chemex) was inductively coupled to the reactor through an externally wound copper coil via an L-C matching network (built into the RF generator). The plasma power (*W*) was balanced by adjusting the matching network to give a minimum reflected power.

Polymerizations typically took 10 min and the polymer film that was produced was collected on aluminium foil, unless otherwise stated. The foil was rinsed thoroughly with Aristar grade methanol (Aldrich), and was then placed horizontally on a glass slide in a central position in the reactor. After 10 min, a film which was sufficiently thick to 'hide' the substrate signal in the subsequent X.p.s. analysis was obtained.

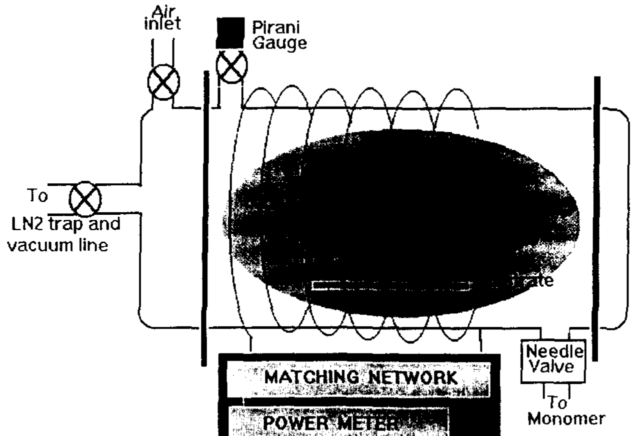

**Figure 1** Schematic diagram of the plasma apparatus

Trifluoroacetic anhydride (TFAA) was obtained from Fluka.

### *Thermal and washing experiments*

Two PP samples, one prepared at a low monomer flow rate, and the other at a higher monomer flow rate, were processed by heating at 100°C under argon. Processing did not contaminate the PPs—this will be discussed later. Further samples of these polymers (deposited on to clean glass) were washed vigorously in distilled water.

### *U.v. irradiation experiments*

Samples were irradiated in air for up to 49 h, at a distance of 10 mm from the cylindrical axis of a Philips LTD 18W/08 black lamp. The output of this lamp is in the range $\lambda = 300$–$410\,\mathrm{nm}$, and in this respect it mimics natural sunlight in the near-u.v. region. The lamp is rated at a power of 18 W. X.p.s. analyses were made on samples taken from the polymers at intervals throughout the programme, with a fresh sample being used for each X.p.s. measurement.

## ANALYSIS

### *X-ray photoelectron spectroscopy (X.p.s.)*

X.p.s. analyses of the PPs were carried out on a VG CLAM 100 photoelectron spectrometer, with MgK$\alpha$ X-rays being used throughout this study. A wide-scan (0–1100 eV) spectrum was recorded, together with the C 1s, oxygen (O 1s) and fluorine (F 1s) regions. The analyser was operated in the fixed analyser transmission (FAT) mode with a pass energy of 100 eV for wide scans and 20 eV for narrow scans. Spectra were peak-fitted using a VGS 5000 data system, on which the spectra were stored. Typical pressures in the analysis chamber during this work were in the region of $10^{-8}$ torr.

### *Monochromated high resolution X.p.s.*

A derivatized PP was analysed on a Scienta ESCA300 spectrometer. This instrument combines a high power (maximum 8 kW) rotating anode and a monochromatized X-ray source (AlK$\alpha$), with high transmission electron optics and a multichannel detector. An electron flood gun was used to achieve charge compensation. This system allows the acquisition of high resolution, high intensity spectra with minimal sample damage. The design and performance of this system has been previously described in full in the literature[25,26].

### *Hydroxyl derivatization*

Samples of PP were placed in a glass dish, which was put horizontally into a desiccator, and 3 ml of TFAA were injected in to a small glass container, which was then placed beside the PP samples inside the sealed vessel. The TFAA, on evaporation, saturated the atmosphere in the desiccator. After 3 h, the PP samples were removed and dried overnight in a vacuum desiccator. In tests carried out using poly(vinyl alcohol), the TFAA was shown by X.p.s. to label 100% of surface hydroxyl groups under these experimental conditions.

### *Time-of-flight secondary ion mass spectrometry (TOF s.i.m.s.)*

The s.i.m.s. analyses were carried out by using a VG Ionex 23LS spectrometer, which was fitted with a pulsed gallium ion source. This instrument has been previously described in the literature[27]. The instrumental conditions were optimized to obtain the maximum count rate, and charge compensation was used as required. All analyses were carried out in the static regime, i.e. with an ion dose $< 10^{13}$ ions cm$^{-2}$ (ref. 28). The spectra were obtained as plots of ion counts against $m/z$ (where $m$ = mass and $z$ = charge of the ion). Both positive and negative ion spectra were recorded.

## RESULTS AND DISCUSSION

### *X.p.s.*

Plasma polymers of allyl alcohol were produced under a range of different monomer flow rate conditions, using a r.f. power of 10 W in each case. Each sample was divided into two parts, one of which was directly analysed by X.p.s., while the other was subjected to trifluoroacetic anhydride derivatization before analysis. The C 1s spectra of the underivatized polymers generally consisted of four components: $\underline{\mathrm{C}}\mathrm{H}$ (referenced to 285.0 eV), $\underline{\mathrm{C}}$–O (286.5 eV), $\underline{\mathrm{C}}$=O (287.7 eV), and a very small amount of O–$\underline{\mathrm{C}}$=O (289.0 eV). We had previously thought that derivatization would introduce just two further peaks at ~290–290.5 and ~293–293.5 eV, corresponding to $\underline{\mathrm{C}}(=\mathrm{O})\mathrm{CF}_3$ and $\underline{\mathrm{C}}\mathrm{F}_3$, respectively. However, as noted in the Introduction, using peaks for $\underline{\mathrm{C}}\mathrm{H}$, $\underline{\mathrm{C}}$–O, $\underline{\mathrm{C}}$=O, O–$\underline{\mathrm{C}}$=O, $\underline{\mathrm{C}}(=\mathrm{O})\mathrm{CF}_3$ and $\underline{\mathrm{C}}\mathrm{F}_3$ of constant full width half-maximum (f.w.h.m.), at the known binding energies of these functionalities, we were not able to obtain chemically acceptable fits for the C 1s core levels of the labelled PPs. This problem was investigated by using the high resolution capability of the Scienta ESCA300 machine. Presented in *Figure 2*, is the C 1s core level spectrum of a labelled PP. In order to obtain the fit shown, it was necessary to use additional peaks for $\beta$-shifted $\underline{\mathrm{C}}\mathrm{H}_2$ and labelled $\underline{\mathrm{C}}$–O. The corrected binding energies for the peaks are given in *Table 1*. A full justification for the use of these additional peaks has been presented elsewhere[18]; for the purpose of this study, it is sufficient to note that the Scienta data indicates their presence and position. Subsequently, eight peak fits were employed to fit the C 1s core-level spectra of the labelled PPs that were obtained on the non-monochromated X.p.s. spectrometer.

The results obtained from the PPs, both before and after derivatization, are given in *Table 2*. In *Table 3*, the

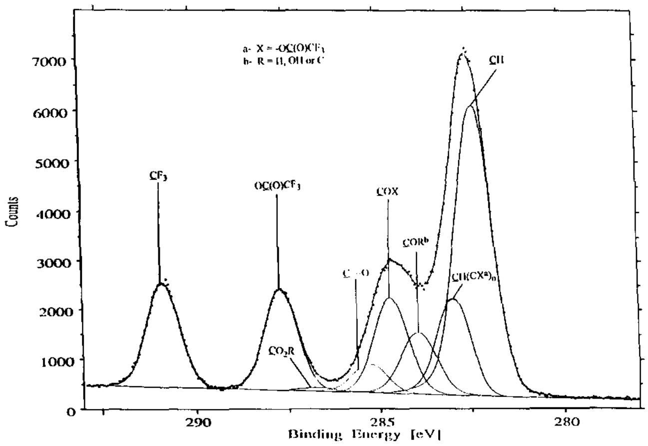

**Figure 2** Labelled PP C 1s core-level fit using additional peaks for $\beta$-shifted $\mathrm{CH}_2$ and labelled C–O: corrected binding energies for the 8 peaks are given in *Table 1*

concentrations of hydroxyl groups found in the polymers per 100 carbon atoms are given, along with the percentage retention of hydroxyl groups (related to the composition of the monomer). The hydroxyl group retention was calculated by dividing the intensity of the $-\underline{C}F_3$ peak in the labelled sample by the total carbon intensity in the same spectrum (minus the contributions of the $-\underline{C}F_3$ and $\underline{C}(=O)CF_3$ peaks, which were not part of the original polymer). At a flow rate of 0.8 cm$^3$(stp) min$^{-1}$, only 14% of the hydroxyl groups were retained, giving a concentration of just 4.5 per 100 carbon atoms, whereas at a flow rate of 2.6 cm$^3$(stp) min$^{-1}$ the degree of retention was 64%, giving a concentration of 21 per 100 carbon atoms. The change-over between conditions that gave rise to PPs with high and low degrees of hydroxyl retention occurred over a relatively narrow range of flow rates namely between 1.7 and 2.6 cm$^3$(stp) min$^{-1}$, as shown in *Figure 3*.

The retention at 2.6 cm$^3$(stp) min$^{-1}$ appears to be the highest obtainable, as the PPs formed at higher flow rates were found to retain slightly fewer hydroxyl groups. The figure of 21 hydroxyl groups per 100 carbon atoms given above is actually an average of several experiments carried out at this flow rate. The highest concentration of hydroxyls obtained in any one experiment was 23 per 100 carbon atoms, corresponding to a degree of retention of 69%. PPs prepared by using a monomer flow of 2.6 cm$^3$(stp) min$^{-1}$ had retained nearly 100% of the oxygen of the monomer.

For a given r.f. power, an increase in the monomer flow rate means that less power is available per unit monomer (lower $W/F$), leading to less fragmentation of the monomer in the plasma. At low flow rates, much more power is available per molecule, and much more fragmentation of the monomer may take place, leading to PPs that may bear little resemblance to their starting monomer. Increasing the monomer flow rate reduces the power available per monomer, and, therefore, minimizes monomer fragmentation in the plasma. A flow rate of 2.6 cm$^3$(stp) min$^{-1}$ probably represents a fairly mild plasma. The results reported in *Table 3* support our argument, although the reason for the decrease in

**Table 1** Corrected C 1s binding energies obtained from derivatized PPs

| Chemical functionality | Corrected binding energy (eV) | Chemical shift (eV) |
|---|---|---|
| $\underline{C}H$ | 285.00 | 0.00 |
| $\underline{C}H(CX)_n$[a] | 285.59 ($n=1$) | 0.59 |
| $\underline{C}OR$[b] | 286.59 | 1.59 |
| $\underline{C}OX$ | 287.35 | 2.35 |
| $\underline{C}=O$ | 287.90 | 2.90 |
| $\underline{C}O_2R$ | 289.30 | 4.30 |
| $O\underline{C}(=O)CF_3$ | 290.33 | 5.33 |
| $\underline{C}F_3$ | 293.52 | 8.52 |

[a] $X=-O\underline{C}(O)CF_3$
[b] R = H, OH or C

**Table 3** Retention of hydroxyl groups

| Flow rate (cm$^3$(stp)min$^{-1}$) | Hydroxyls per 100 carbons | Retention of hydroxyl groups (%) |
|---|---|---|
| 0.8 | 4 | 13 |
| 1.2 | 7 | 21 |
| 1.7 | 10 | 30 |
| 2.2 | 13 | 40 |
| 2.6 | 21 | 64 |
| 3.1 | 16 | 48 |
| 3.5 | 18 | 56 |

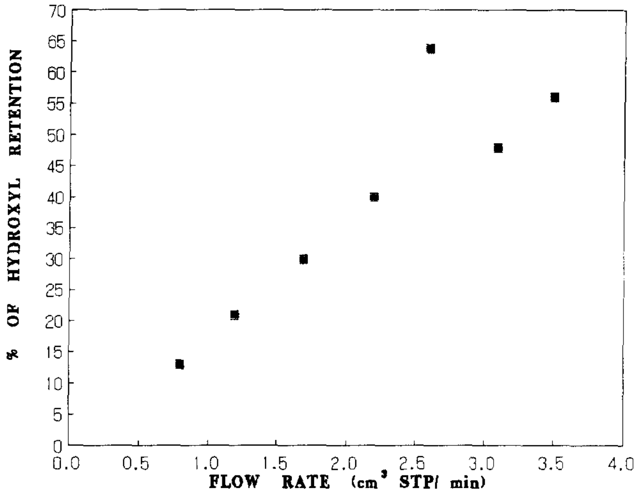

**Figure 3** Hydroxyl retention as a function of the monomer flow rate

**Table 2** X.p.s. data obtained for allyl alcohol plasma polymers[a]

| | | C 1s (%) | | | | | |
|---|---|---|---|---|---|---|---|
| | | Unlabelled | | | | Labelled | |
| Flow rate (cm$^3$(stp) min$^{-1}$) | O/C ratio | $\underline{C}H$ | $\underline{C}-O$ | $C=O$ | $O-\underline{C}=O$ | $\underline{C}(=O)CF_3$ | $\underline{C}F_3$ |
| 0.8 | 0.22 | 70 | 18 | 8 | 4 | 4 | 4 |
| 1.2 | 0.25 | 70 | 22 | 7 | 2 | 6 | 6 |
| 1.7 | 0.22 | 72 | 21 | 6 | 1 | 8 | 8 |
| 2.2 | 0.25 | 70 | 22 | 6 | 1 | 10 | 11 |
| 2.6 | 0.31 | 63 | 31 | 5 | 0 | 15 | 15 |
| 3.1 | 0.29 | 69 | 26 | 5 | 1 | 12 | 12 |
| 3.5 | 0.31 | 63 | 30 | 5 | 1 | 13 | 13 |

[a] The percentages of the components were obtained from the software and do not necessarily equal 100%. The areas of the composite peaks made up from the areas of these components were sometimes slightly more, and sometimes slightly less, than the original core-line area

retention at flow rates greater than 2.6 $cm^3$(stp) $min^{-1}$ is not clear.

The data given in *Tables 2* and *3* may be further used to obtain an estimate of the amount of ether environment in the PPs. For example, in the materials prepared with a flow rate of 2.6 $cm^3$(stp) $min^{-1}$, the ether concentration may be calculated as follows:

1. From the C 1s core-level fit, we know that there are 31 carbons singly bonded to oxygen, and these may be either hydroxyls (C–OH) or ethers (C–O–C). From the labelling results, we know that there are 21 oxygens in hydroxyl environments, so this indicates that there must be 21 carbons in hydroxyl environments.
2. Simple subtraction, therefore, gives that there are 10 carbons in ether environments, or 5 oxygens (since for every oxygen atom there are 2 carbons).
3. This result may be checked. The O/C ratio shows that there are 31 oxygens per 100 carbons. Of these 5 (per 100) are in C=O environments, leaving 26 remaining. Of these, 21 are in hydroxyl environments and, therefore, the remaining 5 must be in ether environments.

For materials prepared using a flow rate of 0.8 $cm^3$(stp) $min^{-1}$, the calculation is complicated by the presence of carboxylate enviroments (4 per 100 carbons). This environment incorporates both ester ($\underline{\mathrm{C}}$(=O)–O–C) and acid ($\underline{\mathrm{C}}$(=O)–OH). The former will also contribute to the $\underline{\mathrm{C}}$–$\bar{\mathrm{O}}$ signal. In order to obtain an estimate of the amount of ether in the PP, a number of assumptions have to be made. The first is that this PP does not contain species other than hydroxyl, ether, carbonyl, acid or ester. The concentration of ethers may be calculated as follows:

1. From the C 1s core level fit, we know that there are 18 carbons per 100 in a $\underline{\mathrm{C}}$–O type environment.
2. Labelling tells us that $\bar{4}$ of these are hydroxyls, leaving 14 to be identified.
3. These 14 are either ether ($\underline{\mathrm{C}}$–O–C) or ester (C(=O)–O–$\underline{\mathrm{C}}$). From the C 1s core level we also know that the number of $\underline{\mathrm{C}}$(=O)–O–C environments is between 0 and 4.
4. If we assume that there are 4 C(=O)–O–C environments (i.e. no C(=O)–OH), there are 10 carbons in ether environments (or 5 oxygens). If we assume that there are 4 C(=O)–OH environments (i.e. no $\underline{\mathrm{C}}$(=O)–O–C environments) then there are 14 carbons in ether environments (or 7 oxygens).

The implications of these assumptions may be checked by counting the number of oxygens per 100 carbons. In the case of no acid, there are 4 oxygens in hydroxyl environments, 8 in carbonyl, 5 in ether, and 8 in ester environments (2 oxygens per environment). This gives us a total of 25 oxygens per 100 carbons, compared to an experimentally determined 22 per 100. If we assume no ester, then there are 7 oxygens in ether environments and a total of 27 oxygens per 100 carbons. The result obtained assuming a complete ester environment (i.e. no acid) gives closer agreement to the experimentally determined O/C ratio, indicating that this is more likely to be the case. The fact that the number of oxygens calculated from the C 1s core level fit is not in agreement with the O/C ratio is more probably a reflection on the accuracy of the C 1s core-level fit than anything else.

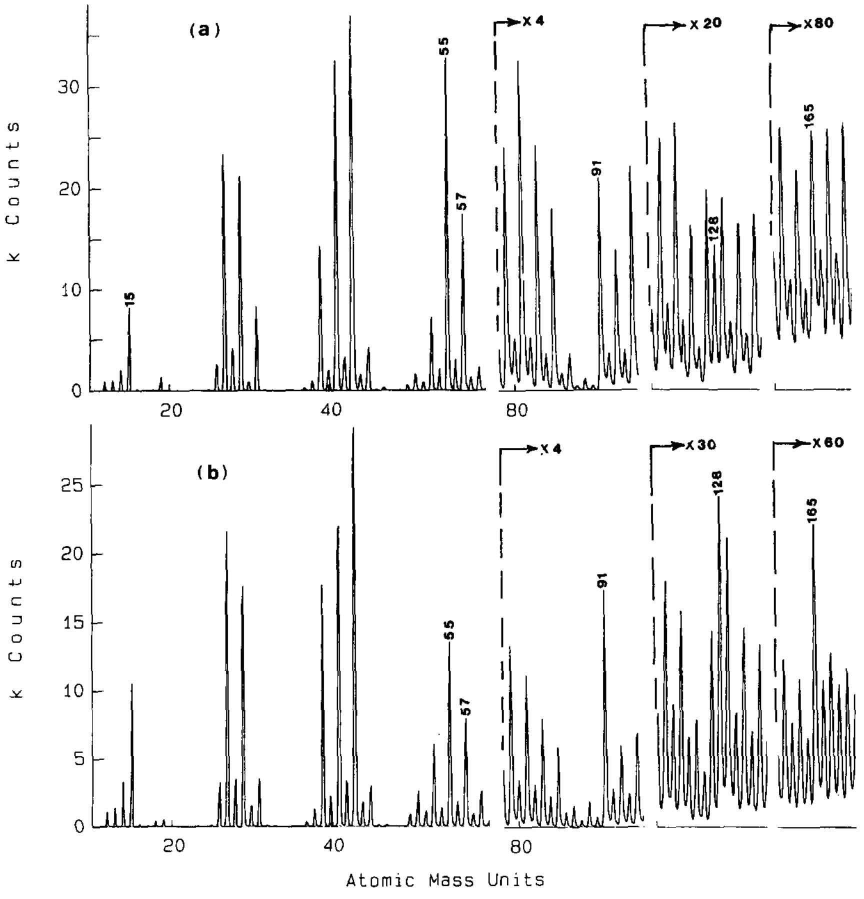

**Figure 4** Positive-ion s.i.m.s. spectra of PPs prepared using different monomer flow rates: (a) 3.5 $cm^3$ (stp) $min^{-1}$; (b) 0.8 $cm^3$ (stp) $min^{-1}$

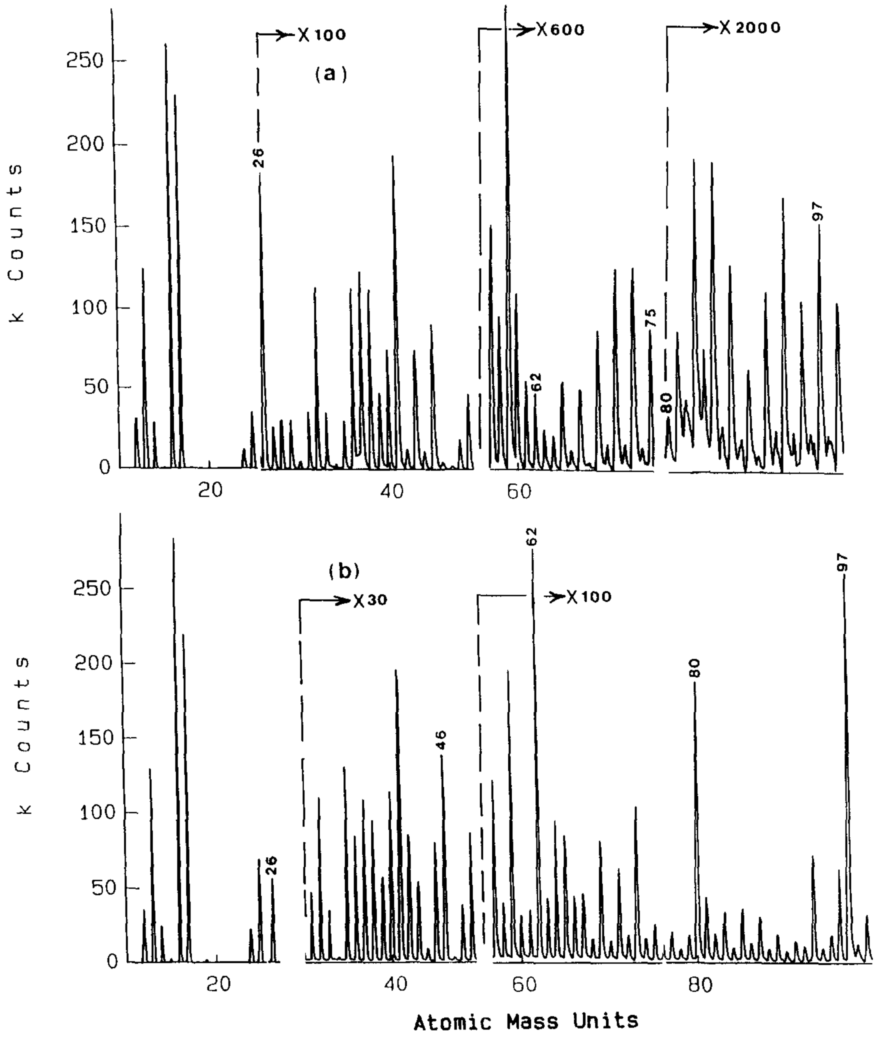

**Figure 5** Negative-ion s.i.m.s. spectra of PPs prepared using different monomer flow rates: (a) 3.5 cm$^3$ (stp) min$^{-1}$; (b) 0.8 cm$^3$ (stp) min$^{-1}$

*TOF s.i.m.s.*

This technique was used to probe molecular structure in a number of PPs of AA, which were prepared by using low (0.8 cm$^3$(stp) min$^{-1}$) through to high (3.5 cm$^3$(stp) min$^{-1}$) monomer flow rates. Despite the difference in hydroxyl concentrations seen across this range, i.e. 13% at 0.8 cm$^3$(stp) min$^{-1}$, and 64% at 2.6 cm$^3$(stp) min$^{-1}$, the s.i.m.s. spectra obtained from these PPs were all remarkably similar. *Figure 4* shows the positive TOF s.i.m.s. spectra recorded for PPs prepared by using monomer flow rates of 3.5 and 0.8 cm$^3$(stp) min$^{-1}$ while *Figure 5* shows the corresponding negative-ion spectra.

In refs 21 and 22, we used the s.i.m.s. spectra from conventional methacrylate polymers to help in the analyses of the s.i.m.s. spectra of their respective PP analogues. In this present case, spectra from conventional analogues were not available. However, the spectra of poly(vinyl alcohol) (PVA) and poly(ethylene oxide) (PEO) have been run on our spectrometer. While the stoichiometry and molecular weight of the repeat units (M) of these polymers are the same, the bonding differs, as shown below:

$$\underset{\text{PEO}}{-(-CH_2CH_2O-)-} \qquad \underset{\text{PVA}}{-(-CH_2CH(OH)-)-}$$

*Positive ions.* Before considering the s.i.m.s. spectra from the two PPs, we draw attention here to how the difference in bonding in PEO and PVA manifests itself in the low-mass positive ions. Displayed in *Figure 6* are the low-mass ($m/z = 0$–$100$) positive-ion spectra for PVA and PEO. In the PVA spectrum, the base peak is the $m/z = 43$ ion, with only a small signal at $m/z = 41$. These ions correspond to $(M-H)^+$ and $(M-3H)^+$, respectively. The $(M+H)^+$ ion at $m/z = 45$ has negligible intensity. However, in the positive-ion s.i.m.s. spectrum of PEO, the most intense peak is at $m/z = 45$ $(M+H)^+$, with only a modest signal from the $m/z = 43$ ion.

Elsewhere[22], we have shown how changes in molecular structure can be identified from the s.i.m.s. spectra, by using a simple numerical normalization procedure. This procedure involves normalizing the area under the peak of interest by the total signal detected, or by the signal of the region in which the peak is located. The molecular weight of AA is 58 Da, and it differs from vinyl alcohol by 14 Da (i.e. $CH_2$). The monomer structures are compared below:

$$\underset{\text{AA}}{CH_2{=}CHCH_2(OH)} \qquad \underset{\text{VA}}{CH_2{=}CHOH}$$

The $(M-H)^+$ ion, seen prominently in PVA, would have a mass of 57 Da in a 'conventional' polymer of AA,

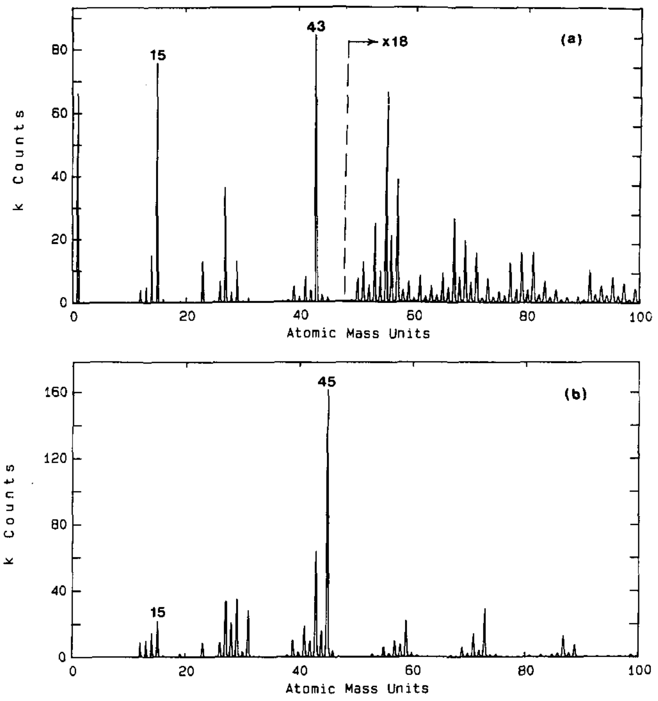

**Figure 6** Low-mass s.i.m.s. positive-ion spectra of (a) PVA and (b) PEO

while the ion at $(M+H)^+$, seen prominently in PEO, would appear at $m/z=59$ with the addition of $CH_2$. Normalization was applied to the s.i.m.s. spectra of the two PPs displayed in *Figure 4*. Signals from the ions corresponding to $(M+H)^+$ and $(M\text{–}H)^+$ ($m/z=59$ and 57) were normalized by the total signal in the range $m/z=50$–100, and the results are displayed in *Table 4*.

The PP prepared using the higher flow rate showed good retention of hydroxyl, which suggests that incorporation of the monomer into the PP occurred through the opening up of the carbon–carbon double bond. This would leave the hydroxyl substituent intact and available for labelling. Support for this view is provided by the results in *Table 4*, which show that the normalized signal at $m/z=57$ is 30% higher in the spectrum of this PP, than in the spectrum of the other PP (which showed low hydroxyl retention). However, the PP with low hydroxyl retention did show reasonable oxygen retention (66%), suggesting (perhaps) that most oxygens were incorporated into the polymer network. This hypothesis is given some credence by the much higher value of the normalized $(M+H)^+$ ion ($m/z=59$), determined from the spectrum of this PP (see *Table 4*).

From the positive-ion spectra, information can also be obtained on the structures that give rise to aromatic fragments (in the s.i.m.s.). The normalized intensities of four of these ions ($m/z=77$, 91, 128 and 165) have been tabulated (*Table 4*). (It should be noted that the ions at $m/z=128$ and 165 were normalized by the range $m/z=110$–180.) These ions are reported in the s.i.m.s. spectra of polystyrene (PS)[29] and have been assigned to cyclic aromatic structures. The detection of these ions does not imply that cyclic aromatic structures existed in the PPs, but, rather structures which could give rise to these ions were present in the PPs. (These original structures were not necessarily aromatic themselves.)

It is worth commenting here that there is some doubt about how these aromatic structures form. Leggett and Vickerman[29] report the observation of aromatic ions, termed polycyclic aromatics (PCAs), at low ion doses in PVC and PMMA, before significant surface modification was achieved. Furthermore, the ion intensities that were monitored did not increase over the dose regime investigated, which suggests (to us) that the concentration of species giving rise to these ions did not increase with ion dose. Our own data are in contrast to these results: we have followed the ion beam induced degradation of PMMA using TOF s.i.m.s. The results obtained indicate that: (1) in the positive ions, at the edge of the static regime there was loss of structures that give rise to PMMA diagnostic ions ($m/z=41$, 59, 69, etc.); (2) there was an increase in the concentration of structures that give rise to aromatic ions ($m/z=77$, 91); and (3) in the negative ions, there was loss of structures that give rise to the diagnostic PMMA ions from $10^{11}$ ions cm$^{-2}$ (see ref. 30).

From the normalized intensities it can be appreciated that the concentration of the four ions referred to above ($m/z=77$, 91, 128 and 165) were much greater in the PP prepared at the lower flow rate (higher *W/F*), suggesting a less regular polymer with more crosslinking. A very similar trend has been seen in plasma-polymerized methacrylates[20]. Generally, PPs are considered to be network polymers, with high crosslink densities. Only by employing low *W/F* conditions, for example by using high monomer flow rates, can PPs with good functional group retention be obtained. The observed increase in 'aromaticity' occurred with loss of functional group (as determined by X.p.s.), and fits well with the idea that at higher *W/F* values there was much greater fragmentation and rearrangement in the monomer.

*Negative ions.* At low mass, the negative s.i.m.s. spectra of PVA and PEO are remarkably similar: both contain strong $m/z=43$ ions $(M\text{–}H)^-$, with intense $m/z=41$ ions (M–3H); neither show any appreciable $m/z=45$ ions $(M+H)^-$. For this reason, they are not shown. The polymers can be distinguished by a series of ions corresponding to $HO\text{–}(M)_nCH_2CH_2O^-$ which are seen in the spectrum of PEO, but not seen in PVA. (There is also a strong signal for $m/z=58$ which only appears in the spectrum of PEO.) Some clear differences in the negative-ion spectra for the two PPs of AA were observed (see *Figure 5*); however, we do not believe that these reflect any structural deviations, but, indicate small amounts of contamination in the low-monomer-flow-rate PP. In this PP, the ions at $m/z=26$, 46 and 62 are assigned to $CN^-$, $NO_2^-$ and $NO_3^-$, respectively. The nitrogen probably

**Table 4** Normalized s.i.m.s. positive ion intensities

| Positive ions ($m/z$) | Mass range | Normalized positive ion intensity ($\times 10^3$) at a flow rate (cm$^3$(stp) min$^{-1}$) of 0.8 | 3.5 |
|---|---|---|---|
| 55 | 50–100 | 54.44 | 77.00 |
| 57 | 50–100 | 35.10 | 45.72 |
| 59 | 50–100 | 11.94 | 06.65 |
| 77 | 50–100 | 20.66 | 13.49 |
| 91 | 50–100 | 18.24 | 16.58 |
| 128 | 110–180 | 36.22 | 20.70 |
| 165 | 110–180 | 18.24 | 12.10 |

leaked into the plasma apparatus and was incorporated into the PP during polymerization. Any small leak in the apparatus will naturally be more serious at a low flow rate. Furthermore, the ions at $m/z=80$ and 97 are assigned to $SO_2^-$ and $HSO_4^-$. The source of this contamination is unknown. Both PPs showed ions corresponding to $(M-H)^-$, but not $(M+H)^-$.

*Crosslinking and functional group mobility*

The water solubility of the PPs showing the highest and lowest degrees of hydroxyl retention was investigated in a simple washing experiment using distilled water. The samples were prepared on glass to enable easier handling. The X.p.s. spectra (both before and after washing) of the high-retention PP are displayed in *Figure 7*. These spectra reveal that a large proportion of the high-retention PP was washed from the glass substrate. Before washing, no substrate signal was seen, while the widescan spectrum of the washed material shows clear silicon signals (Si 2s at 153 eV, and Si 2p at 102 eV) from the glass substrate. Furthermore, both the C 1s and O 1s core levels were substantially altered by washing.

In contrast, little difference was seen in the before, and after washing spectra (widescan and core lines) of the low-retention PP. These spectra are not shown here in order to conserve space. The PP deposit was still sufficiently thick after washing to prevent the detection of the substrate signal, and the shape of the individual core lines were essentially unaltered by washing. We conclude that this material was sufficiently crosslinked to resist washing.

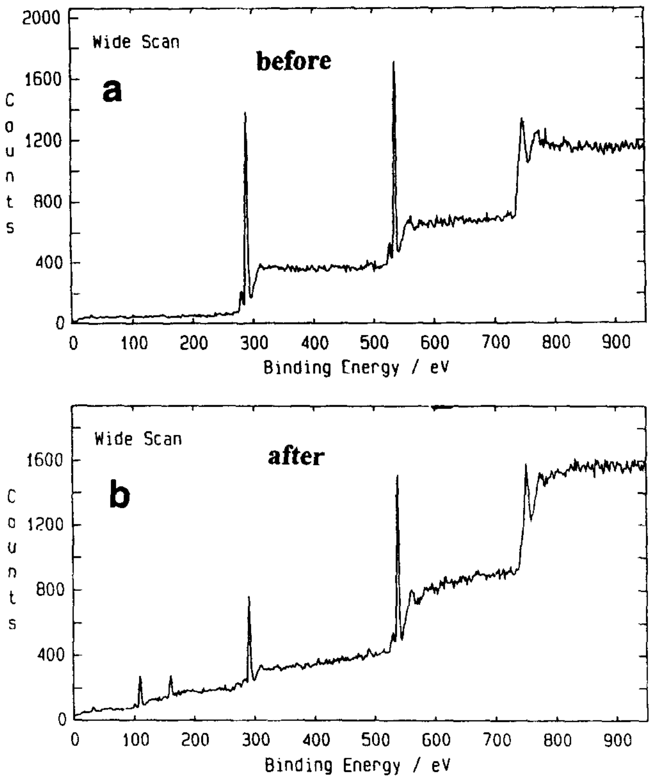

**Figure 7** X.p.s. widescan spectra of the high-retention PP (a) before and (b) after washing

The washing data reveal that the high-retention PP either:

(i) contained a soluble fraction, presumably of low molecular weight (low crosslinking) or;
(ii) the material was completely soluble except for a strongly adsorbed layer at the glass surface.

The data also show that the low-retention PP was sufficiently crosslinked to be insoluble. The idea that the high-retention PP contained at least two different fractions was further explored by annealing this PP and the low-retention PP in a clean oven, under an inert atmosphere, at 100°C. While no changes were observed in the widescan and the C 1s and O 1s core levels of the low-retention PP after heating, changes had occurred in the spectra of the high-retention material. Comparison of the before and after X.p.s. spectra reveal loss of oxygen (widescan) and of oxidized carbon functionalities (C 1s) from the surface of the PP. These changes have been quantified and are given in *Table 5*.

The data show that the low-retention PP was unaffected by this processing, as well as confirming the cleanliness of the oven. The data in *Table 5* also reveal that substantial changes had taken place in the surface of the high-retention PP. One of two events may have occurred:

(i) sample degradation;
(ii) surface reorganization, involving migration and/or reorientation of a more hydroxyl (oxygen)-rich fraction of the material away from the air–polymer interface.

The first possibility is considered to be the less likely in the light of the u.v. (stability) data which are presented below. Taken together, the washing and thermal treatment results point to the high-retention PP being of low molecular weight (low number of crosslinks), and containing oxygen-rich and less-oxygen-rich fractions. The oxygen-rich fraction is mobile and on heating the sample migrates/reorientates away from the polymer surface. The low–retention PP is more highly crosslinked and can resist washing and surface reorganization.

*U.v. experiment*

When the high and low-retention PPs were exposed to a low-intensity u.v. source, a dramatic difference in the responses of these two materials was observed. The surface O/C ratios of these two types of materials after

**Table 5** X.p.s. data for allyl alcohol plasma polymers before and after heating in argon

| Condition | Flow rate ($cm^3$(stp) $min^{-1}$) | O/C ratio | Amount of environment (%) in C 1s core level | | | |
|---|---|---|---|---|---|---|
| | | | CH | C–O | C=O | C(=O)OH/R |
| Before heating | 0.8 | 0.22 | 64 | 22 | 10 | 4 |
| After heating | 0.8 | 0.21 | 66 | 21 | 10 | 3 |
| Before heating | 2.6 | 0.27 | 68 | 26 | 6 | 0 |
| After heating | 2.6 | 0.21 | 72 | 22 | 6 | 0 |

**Table 6** O/C surface ratios in allyl alcohol plasma polymers before and after exposure to u.v. irradiation

| Flow rate (cm(stp) min$^{-1}$) | % of O/C<br>Before u.v. exposure | After exposure to u.v. for<br>19 h | <br>49 h |
|---|---|---|---|
| 2.6 | 0.27 | 0.25 | 0.25 |
| 0.8 | 0.21 | 0.27 | 0.29 |

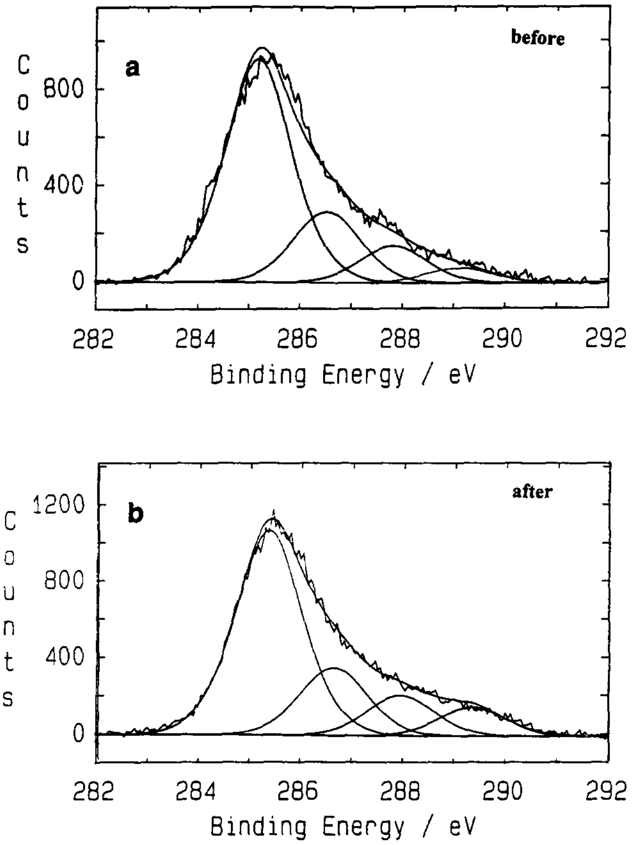

**Figure 8** C 1s core lines of the low-retention PP (a) before and (b) after 49 h of u.v. exposure

19 and 49 h exposure are given in *Table 6*. The results show that the low-retention PP progressively took up oxygen, while the high-retention PP did not. The C 1s and O 1s core lines of the high-retention PP were essentially unaffected by the u.v. irradiation and, hence, we conclude that this material was stable over the period of investigation. In the low-retention PP, concomitant with oxygen uptake, in the C 1s core line there was a small, but significant, increase in the signal to the high binding energy side of the C–H peak. This indicates that u.v. exposure had produced an increase in the number of oxidized carbons (C–O, O–C–O, C=O and O–C=O), which can be seen in *Figure 8*. The results obtained by peak-fitting the spectra in this figure are given in *Table 7*.

We attribute the differences in response of these materials to a higher concentration of free-radicals in the low-retention PP. It is well known that PPs contain a high density of trapped free-radicals ($10^{17}$–$10^{20}$ spins per cubic centimetre)[10]. These free-radicals may be trapped in the PP during formation, or formed by the impingement of energetic particles on the surface of the polymer deposit, or by u.v. from the plasma. From a knowledge of the mechanisms of thermal and oxidative degradation in conventional polymers, we suspect that PPs may not be particularly stable to environmental agents, e.g. heat and light, although little has been written on this subject. In ref. 24, we reported that PPs of methyl methacrylate (MMA) and styrene photo-oxidized rapidly when compared to their conventional analogues. Here, we show that the rate of oxygen uptake is dependent on the plasma preparation conditions that are employed. We are not aware of any work on the relationship between *W*, *F* and the trapped free-radical density concerning the AA monomer. The relationship observed with other monomers is complex (i.e. it is dependent on the monomer studied). With most systems, an increase in the *W*/*F* ratio results in a higher concentration of residual free-radicals trapped within the polymer deposit, although there are several notable exceptions. When PPs of MMA, prepared at high and low *W*/*F* ratios, were exposed to u.v. from a 'black lamp', the high *W*/*F* materials (low functional group retention) were also found to photo-oxidize rapidly, while the low *W*/*F* materials did not[31].

**Table 7** Chemical environments seen in the low-retention plasma polymers of allyl alcohol before and after u.v. exposure

| Peak no. | Chemical environment | Peak intensity (area %)<br>Before u.v. exposure | <br>After exposure to u.v. for 49 h |
|---|---|---|---|
| 1 | $\underline{C}H$ | 65 | 60 |
| 2 | $\underline{C}OR^a$ | 20 | 20 |
| 3 | $\underline{C}{=}O$ | 11 | 12 |
| 4 | $\underline{C}O_2R$ | 4 | 8 |

$^a$R=H, OH or C

Whether the explanation forwarded here for the difference in u.v. stability is correct or not, the data reported have important implications if PPs of AA are to be used in an environment where they may be exposed to u.v. irradiation.

### *Surface reactivity*

In an attempt to increase the surface concentration of the hydroxyl groups still further, the flow of monomer over newly formed PPs was allowed to continue for a period of 30 min after the plasma had been switched off. It was thought that this might enable free radicals in the polymer surface to react with the AA monomer. X.p.s. results obtained from PPs prepared at flow rates of 1.7, 2.6 and 3.5 cm$^3$(stp) mm$^{-1}$, however, showed no detectable difference between these and various control samples in which the monomer flow had been stopped immediately after the plasma had been turned off.

### *Plasma polymerization of 1-propanol*

In contrast to AA, PPs of 1-propanol showed very little retention of –OH groups, even under high-flow-rate conditions. At a flow rate of 3.0 cm$^3$(stp) min$^{-1}$, the degree of hydroxyl retention was only 14%. This is likely to be due to elimination of $H_2O$ from the propanol to form propylene, which then undergoes polymerization, as a preferred reaction pathway.

## CONCLUSIONS

Thin surface coatings were formed by the plasma polymerization of AA. These deposits were analysed by X.p.s. with the aid of TFAA labelling. Problems were encountered when fitting the spectra of labelled PPs by just using peaks for $\underline{C}H$, $\underline{C}$–O, $\underline{C}$=O, $\underline{C}O_2H/R$, $\underline{C}(=O)CF_3$ and $\underline{C}F_3$. The high resolution X.p.s. spectra obtained from the derivatized PPs revealed significant chemical shifts in the carbon atoms attached to the $-C(=O)CF_3$ group and those in the $\beta$-position relative to this group. This information was used in the fitting of the lower resolution X.p.s. spectra which were obtained in the bulk of this study.

The reported X.p.s. data show that the coatings contained hydroxyl groups in concentrations up to 23 per 100 carbon atoms (or approximately one for every 4.5 carbon atoms). The highest degree of hydroxyl retention occurred under mild conditions, with a monomer flow rate of $\sim 2.6\,cm^3(stp)\,min^{-1}$. At higher flow rates than this, the retention was somewhat less, while at lower flow rates the concentration of hydroxyl groups in the PPs fell away rapidly.

The TOF s.i.m.s. spectra obtained from the high and low-retention PPs were all remarkably similar. To facilitate comparison, a simple normalization procedure was adopted, whereby the intensity of the ion of interest was normalized by the background signal from the region of the spectrum in which it was located. Using this procedure, some evidence was obtained which suggests that in the high-retention PP some monomer repeat units had deposited via a conventional-like mechanism, i.e. through the double bond, while in the low-retention PP, the oxygen in the pendant hydroxyl (of the monomer) was now directly bonded into the polymer network. The low-retention PP also contained a higher concentration of unsaturated moieties, which gave rise to aromatic ions in the s.i.m.s.

Data from washing and thermal treatment of a high-retention PP suggest that the material was of low molecular weight and could undergo substantial surface reorganization, implying that the PP consisted of at least two fractions. A low-retention PP was shown to be resistant to both washing and thermally induced reorganization, suggesting a higher degree of cross-linking. A simple u.v. ageing experiment revealed that the high-retention PP was stable to u.v., while the low-retention PP photo-oxidized rapidly. This behaviour was attributed to a higher concentration of free-radical centres in the material, but an attempt to use these to post-graft AA, in order to increase surface hydroxyl functionality, was unsuccessful.

The importance of the double bond for good hydroxyl retention was further illustrated by the data obtained from the plasma polymerization of 1-propanol. The PPs of 1-proponal did not contain high concentrations of hydroxyl, and this was attributed to the favourable elimination of $H_2O$, even under mild plasma conditions.

## ACKNOWLEDGEMENTS

The authors would like to acknowledge Professor David Briggs and Dr Graham Beamson (ICI, Wilton, UK) for access to the high resolution X.p.s. equipment, and for help with data interpretation. They would also like to thank Dr Morgan Alexander (University of Sheffield) for thinking through the data with us, and the SERC for the grant that made this work possible.

## REFERENCES

1 Gombotz, W. and Hoffman, A. *J. Appl. Polym. Sci.: Appl. Polym. Symp.* 1988, **42**, 285
2 Gombotz, W. and Hoffman, A. *J. Appl. Polym. Sci.* 1989, **37**, 91
3 Heider, G. H., Gerbert, M. B. and Yacynych, A. M. *Anal. Chem.* 1982, **54**, 324
4 Hozumi, K. *Pure Appl. Chem.* 1988, **60**, 697
5 Bradley, A. and Fales, J. *J. Chemtech* 1971, 232
6 Bradley, A. *J. Chemtech* 1973, 607
7 Sanchez Urrutia, M., Schreiber, H. P. and Wertheimer, M. R. *J. Appl. Polym. Sci. Appl. Polym. Symp.* 1988, **42**, 305
8 Inagaki, N. and Matsunaga, M. *Polym. Bull.* 1986, **13**, 349
9 Gangal, S., Hori, M., Yoneda, T., Morita, S. and Hottori, S. ISPC-7, Eindhoven, July 1985
10 Yasuda, H. K. 'Plasma Polymerization', Academic Press, London, 1985
11 Ohno, M., Ohno, K. and Sohma, J. *J. Polym. Sci., Polym. Chem. Edn* 1987, **25**, 1273
12 Everhart, D. S. and Reilley, C. N. *Anal. Chem.* 1981, **53**, 665
13 Dickie, A., Hammond, J. S., Vries, J. E. and Holubka, J. W. *Anal. Chem.* 1982, **54**, 2045
14 Gerenser, L. J., Elman, J. F., Mason, M. G. and Pochan, J. M. *Polymer* 1985, **26**, 1162
15 Briggs, D. and Kendall, C. R. *Int. J. Adh. Adhs.* 1982, **2**, 13
16 Chiltoki, A. and Ratner, B. D. *Surf. Interface Anal.* 1991, **17**, 567
17 Pochan, J. M., Gerenser, L. J. and Elman, J. F. *Polymer* 1986, **27**, 1058
18 Ameen, A. P., Ward, R. J., Short, R. D., Beamson, G. and Briggs, D. *Polymer* 1993, **34**, 1795
19 Ward, R. J. *PhD Thesis*, University of Durham, 1989
20 Ward, A. J., Ameen, A. P. and Short, R. D., unpublished results
21 Ward, A. J. and Short, R. D. *Polymer* 1993, **34**, 4179
22 Short, R. D., Ameen, A. P., Jackson, S. T., Pawson, D. J., O'Toole L. and Ward, A. J. *Vacuum* 1993, **44**, 1143
23 Ward, R. J., Munro, H. S., Davies, M. C. and Short, R. D. *Polymer* 1993, **34**, 2250
24 Potter, W., Ward, A. J. and Short, R. D. *Polym. Degrad. Stability* 1994, **43**, 385
25 Gelius, U., Wannberg, B., Baltzer, P., Fellner-Feldegg, H., Carlson, G., Johansson, C. G., Larson, J., Munger, P. and Vegerfors, G. *J. Electron Spectrosc. Related Phenom.* 1990, **52**, 747
26 Beamson, G., Briggs, D., Davies, S. F., Fletcher, I. W., Clark, D. T., Havard, J., Geluis, U., Wannberg, D. and Baltzer, P. *Surf. Interface Anal.* 1990, **15**, 541
27 Eccles, A. J. and Vickerman, J. C. *J. Vac. Sci. Technol.* 1988, **A7**, 234
28 Briggs, D. and Hearn, M. J. *Vacuum* 1986, **36**, 1005
29 Leggett, G. J. and Vickerman, J. C. *Appl. Surf. Sci.* 1992, **55**, 105
30 Jackson, S. T. *PhD Thesis*, University of Sheffield, 1992
31 Ward, A. J., Potter, W. and Short, R. D. unpublished results, 1992/93